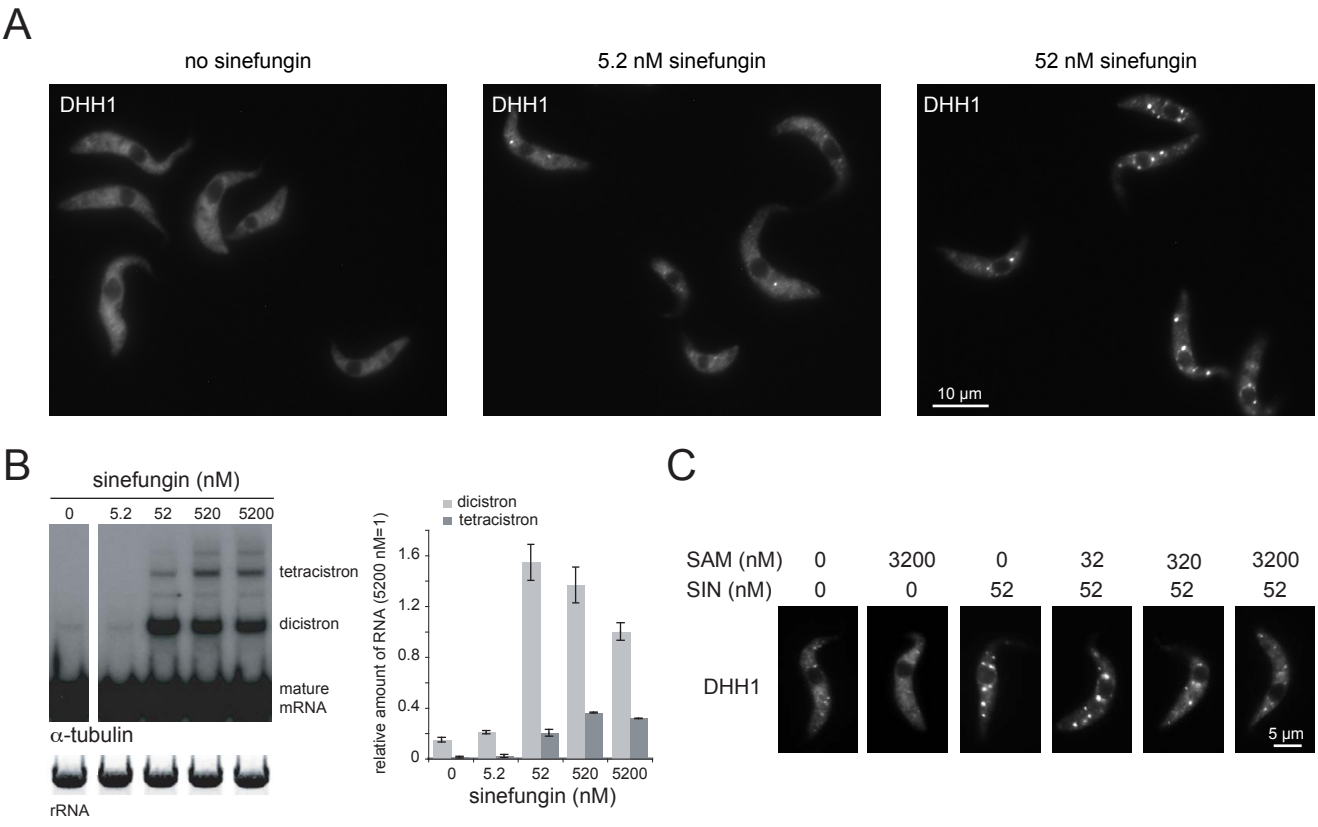

Figure S1
Determination of the threshold concentration(s) of sinefungin required for eYFP-DHH1 localisation to NPGs and inhibition of tubulin mRNA maturation.
(A) Cells were incubated for 60 min and images collected.
(B) Northern blot analysis of incompletely processed tubulin mRNAs from cells treated in the same manner as (A); dicistronic and tetracistronic tubulin mRNAs from three experiments were quantified.
(C) Co-incubation with excess S-adenosyl methionine prevents the sinefungin-induced formation of NPGs. Incubations were for 60 minutes.

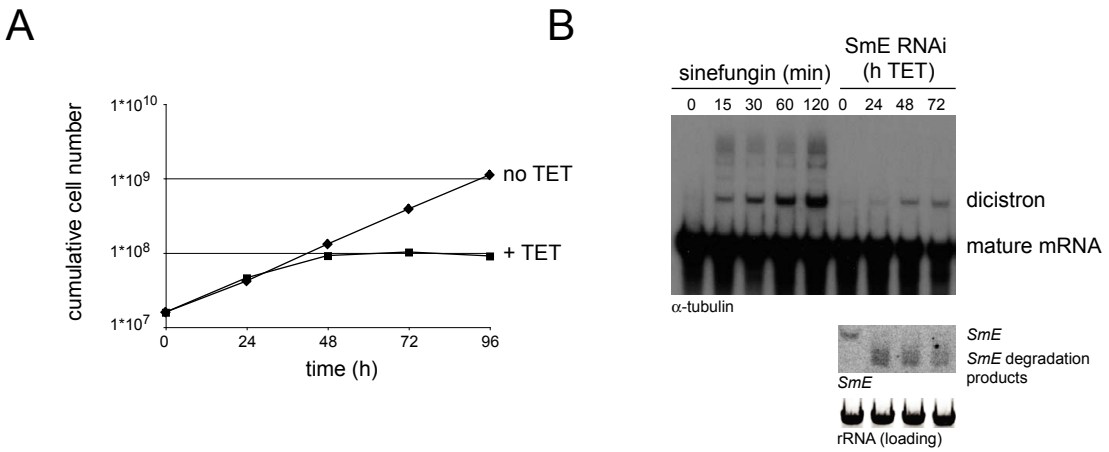

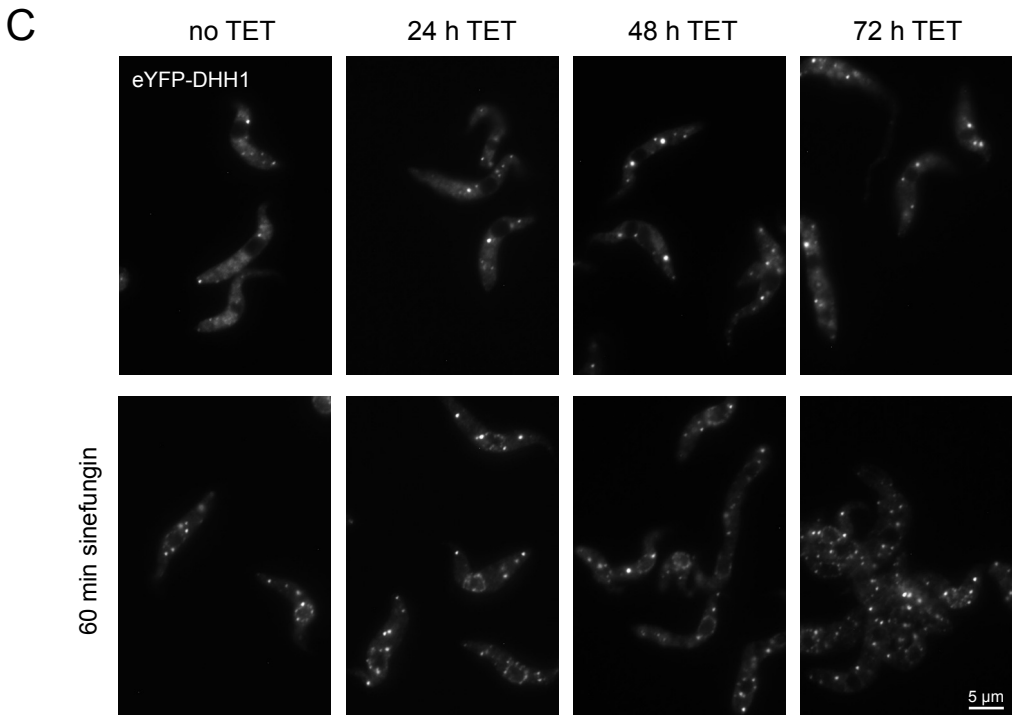

Figure S2
RNAi depletion of SmE does not cause the formation of NPGs
SmE protein was depleted in cells constitutively expressing eYFP-DHH1.
(A) SmE RNAi resulted in reduced proliferation.
(B) Northern blot analysis of incompletely processed tubulin mRNAs (top) and *SmE* mRNA (bottom) over a time course of SmE RNAi compared with the effect of sinefungin (top). Note that SmE RNAi resulted in less accumulation of incompletely processed tubulin mRNA than sinefungin.
(C) Localisation of eYFP-DHH1 over a time course of SmE RNAi and the effect of incubation with sinefungin. Note that SmE RNAi caused an increase in cytoplasmic P-bodies, but no formation of NPGs. Moreover, when SmE depleted cells were treated with sinefungin, NPGs still formed in the majority of the cells.

FIGURE S3

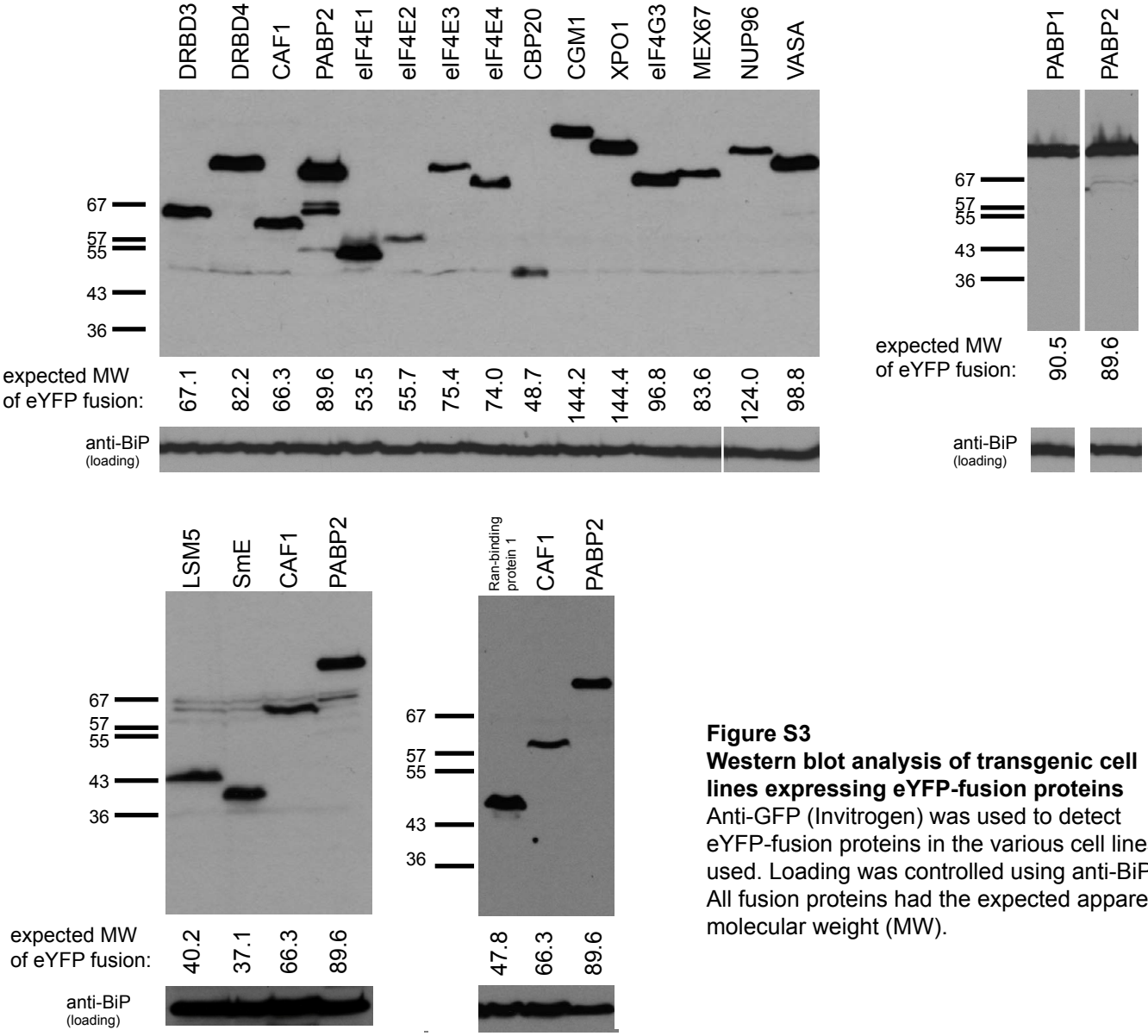

Figure S3
Western blot analysis of transgenic cell lines expressing eYFP-fusion proteins
Anti-GFP (Invitrogen) was used to detect eYFP-fusion proteins in the various cell lines used. Loading was controlled using anti-BiP. All fusion proteins had the expected apparent molecular weight (MW).

FIGURE S4

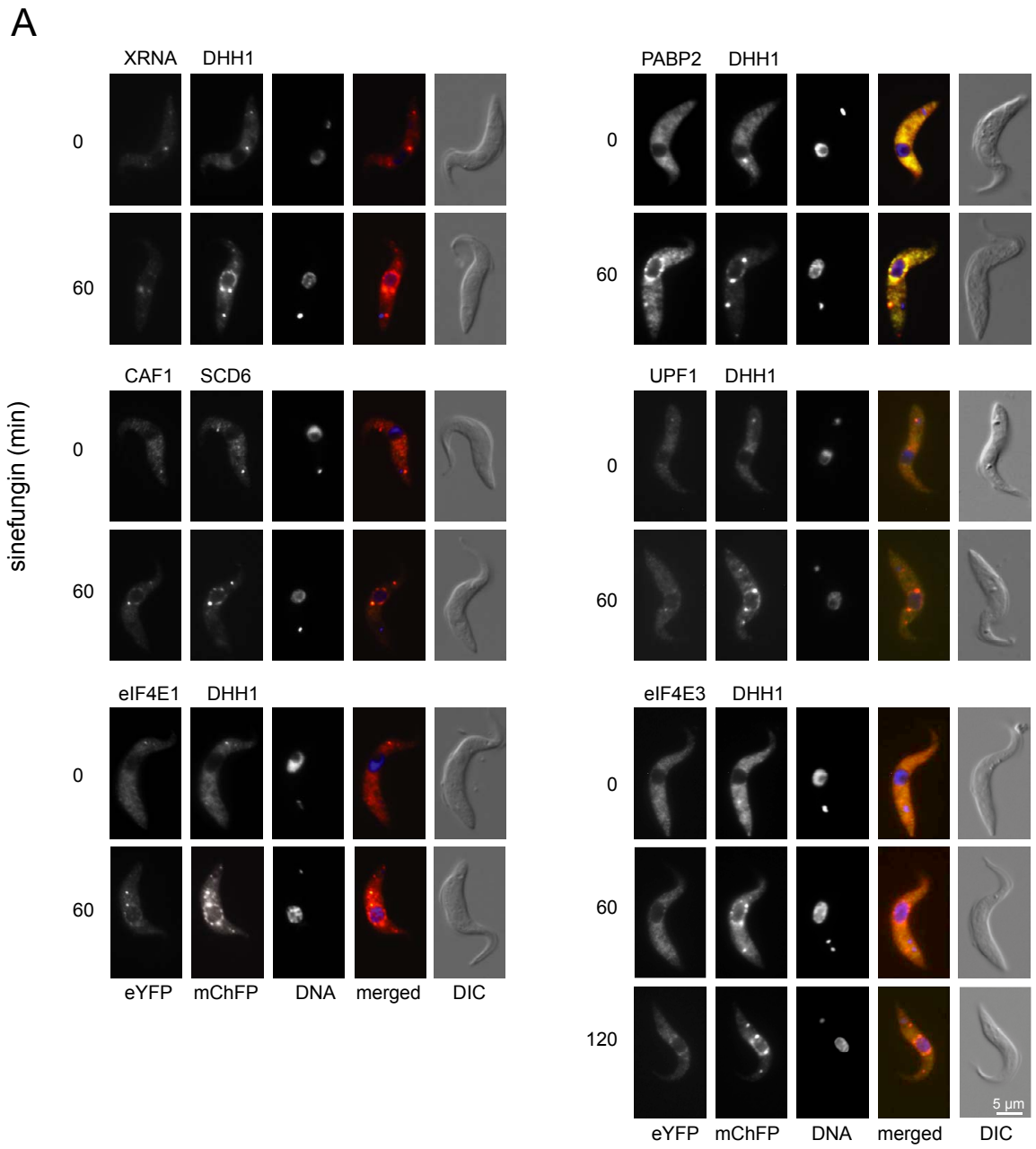
A
sinefungin (min)
XRNA
DHH1
PABP2
DHH1
CAF1
SCD6
UPF1
DHH1
eIF4E1
DHH1
eIF4E3
DHH1
0
60
120
eYFP
mChFP
DNA
merged
DIC
5 µm

FIGURE S4

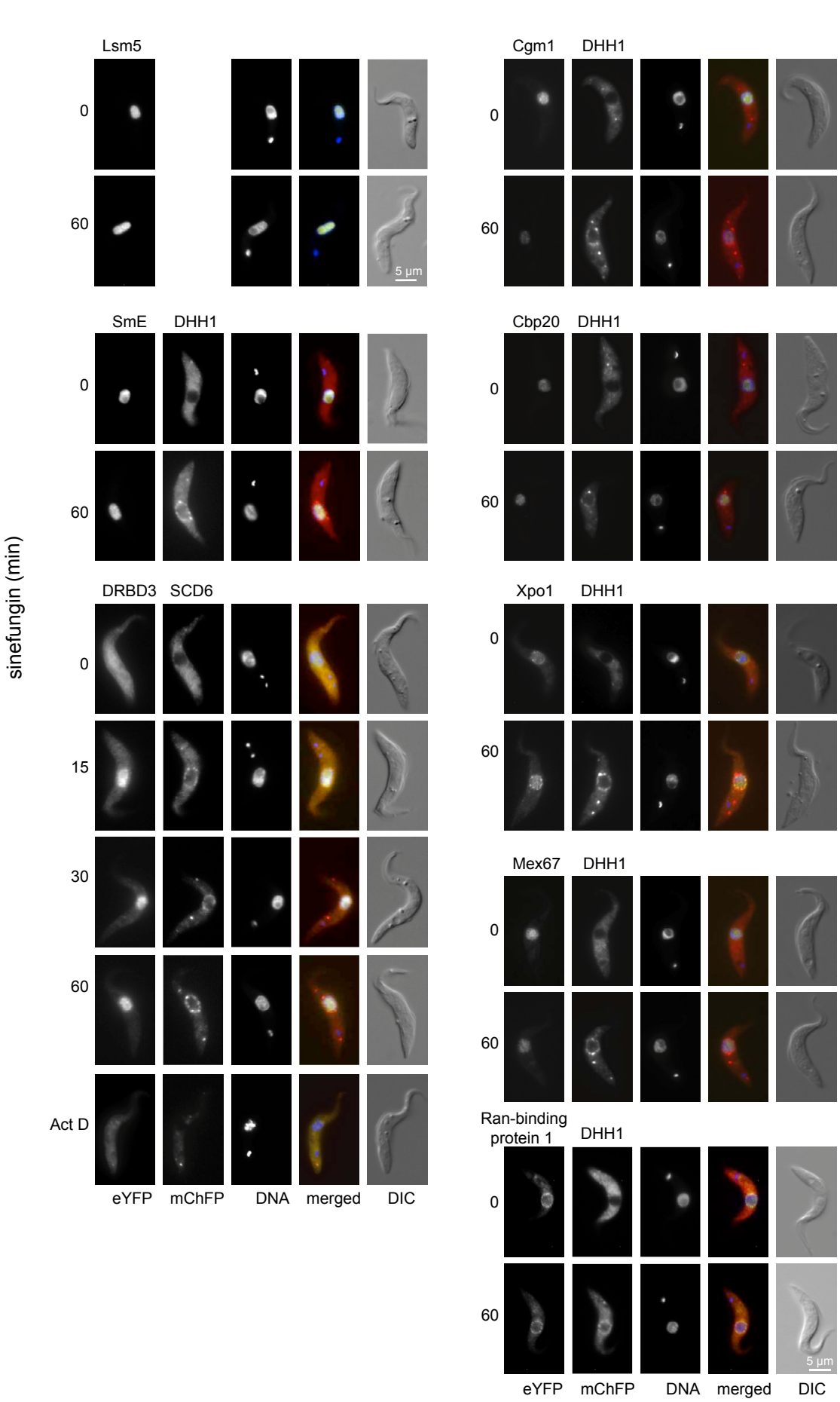
B
Lsm5
Cgm1
DHH1
SmE
DHH1
Cbp20
DHH1
DRBD3
SCD6
Xpo1
DHH1
Mex67
DHH1
Ran-binding protein 1
DHH1
sinefungin (min)
0
15
30
60
Act D
5 µm
eYFP
mChFP
DNA
merged
DIC

B (continued)

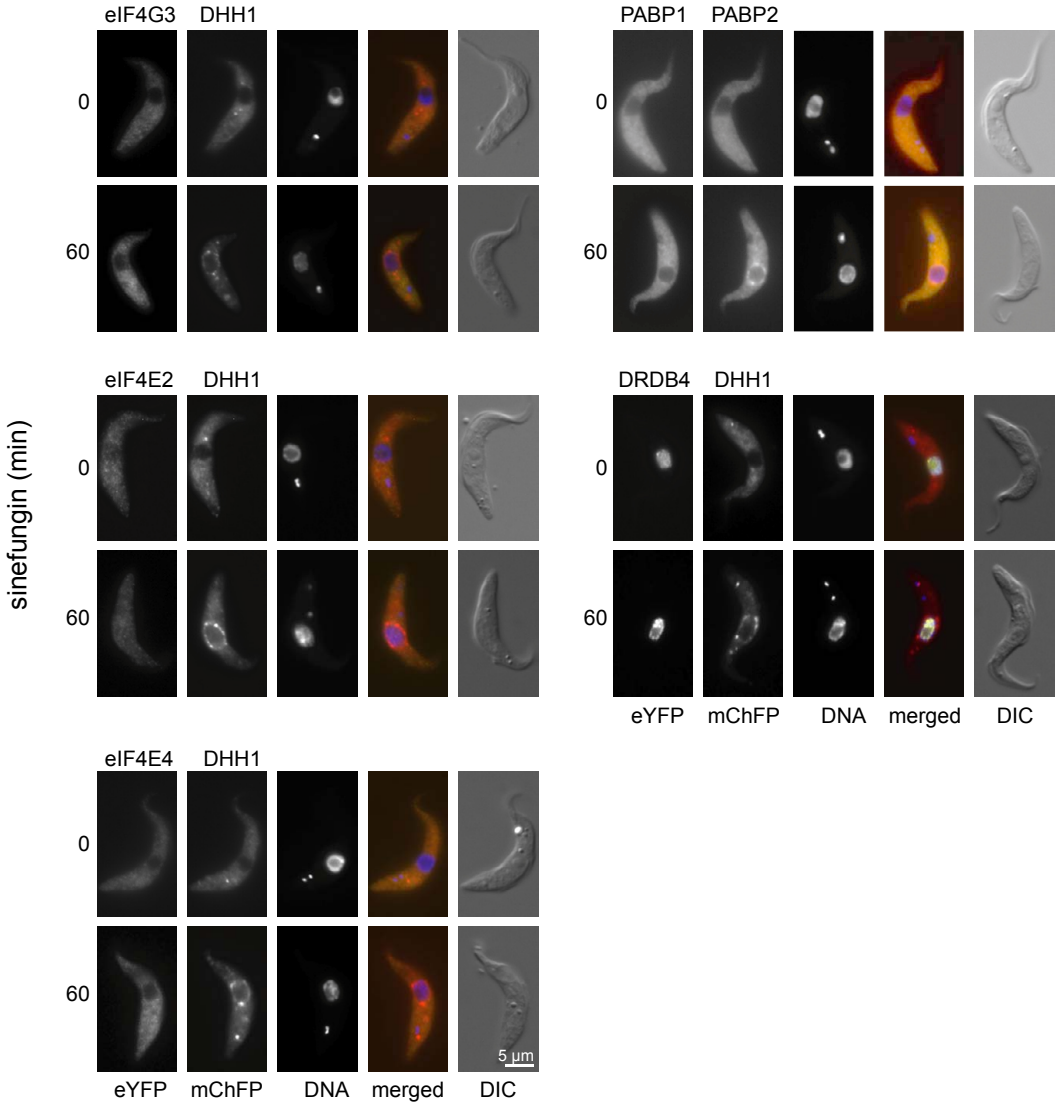

Figure S4
Screen for proteins localizing to NPGs
eYFP-fusions of proteins involved in various aspects of RNA metabolism were co-expressed with an NPG marker protein, either mChFP-DHH1, SCD6-mChFP or PABP2-mChFP. All transgenes, except LSM5-eYFP, were expressed after modification of one endogenous allele. LSM5-eYFP was expressed as a tetracycline-inducible transgene using a pDEX377 derivative (Kelly et al., 2007) in cells without an NPG marker.
Each protein was tested for localisation to NPGs after incubation with sinefungin for 60 min. Cells expressing DRBD3-eYFP were also treated with actinomycin D for 60 min.
A) Proteins that localize to the NPGs
B) Proteins that do not localize to the NPGs

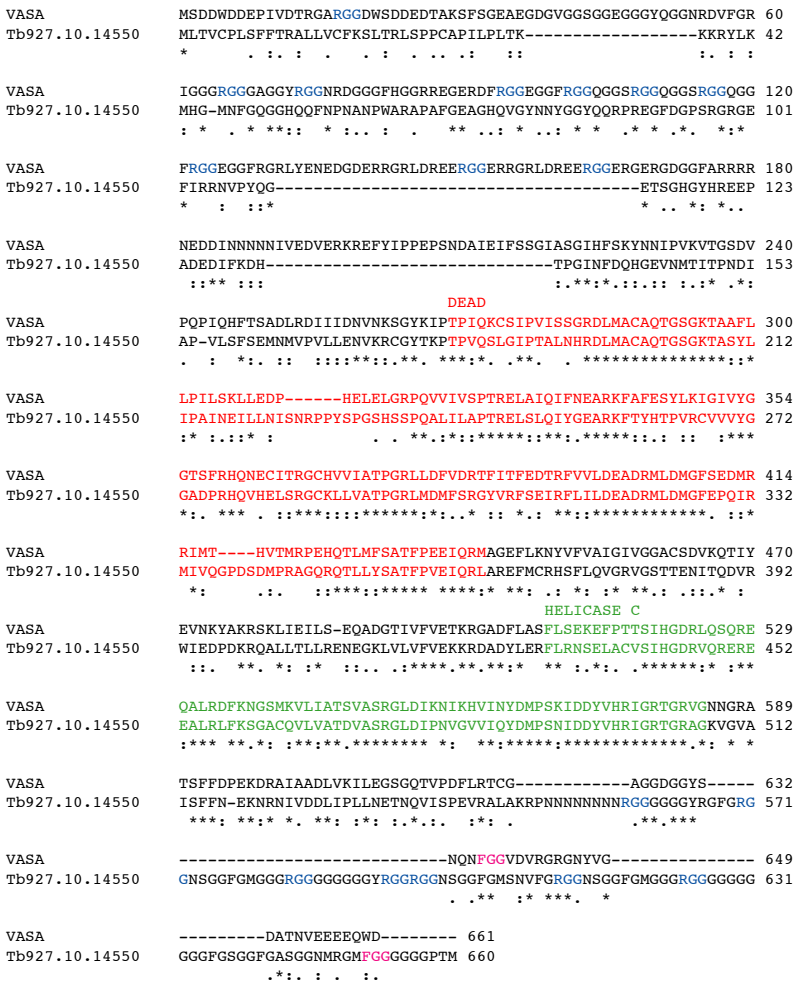

Figure S5
Amino acid sequence alignment of *Drosophila* VASA with its closest *T. brucei* homologue (Tb927.10.14550)
Conserved Pfam motifs are coloured. RRG motifs are coloured in blue and FGG motifs in pink. Both *Drosophila* VASA and the homologous *C. elegans* GLH proteins 1, 2 and 4 possess a glycine-rich domain, but in VASA this domain contains RGG motifs, an established RNA-binding domain (Kiledjian and Dreyfuss, 1992) and in GLH proteins it contains FGG motifs, which interact with nuclear pore components (Suntharalingam and Wente, 2003). The *T. brucei* homologue has seven RGG and one FGG motif in its glycine-rich domain at its C-terminus indicating closer homology to *Drosophila* VASA than to *C. elegans* GLH. The alignment was performed using ClustalW with default settings.

Kiledjian, M. and Dreyfuss, G. (1992). Primary structure and binding activity of the hnRNP U protein: binding RNA through RGG box. *EMBO J* **11**, 2655-64.

Suntharalingam, M. and Wente, S. R. (2003). Peering through the pore: nuclear pore complex structure, assembly, and function. *Dev Cell* **4**, 775-89.

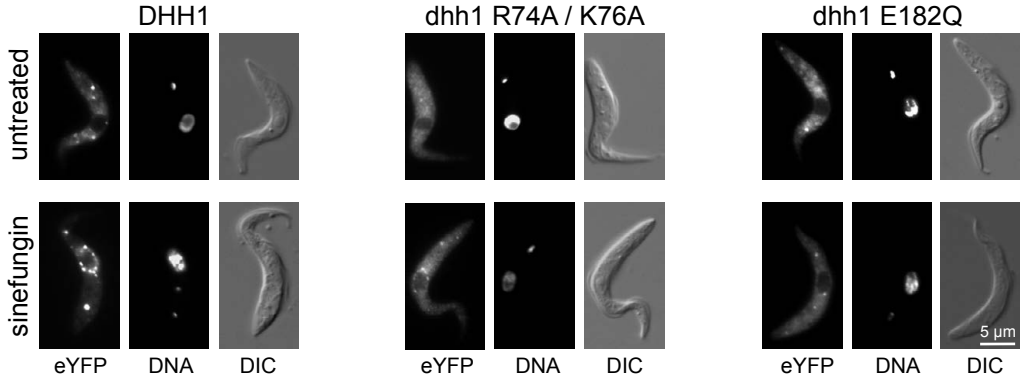

Figure S6
Dhh1 mutant proteins have reduced localization to NPGs
DHH1 mutant proteins impaired in RNA binding (dhh1 R74A/K76A) or ATPase activity (dhh1 E182Q) have reduced localization to P-bodies (Kramer et al., 2010b). Localization of the mutant proteins to NPGs was determined after incubation with sinefungin for 60 min.

FIGURE S7

A

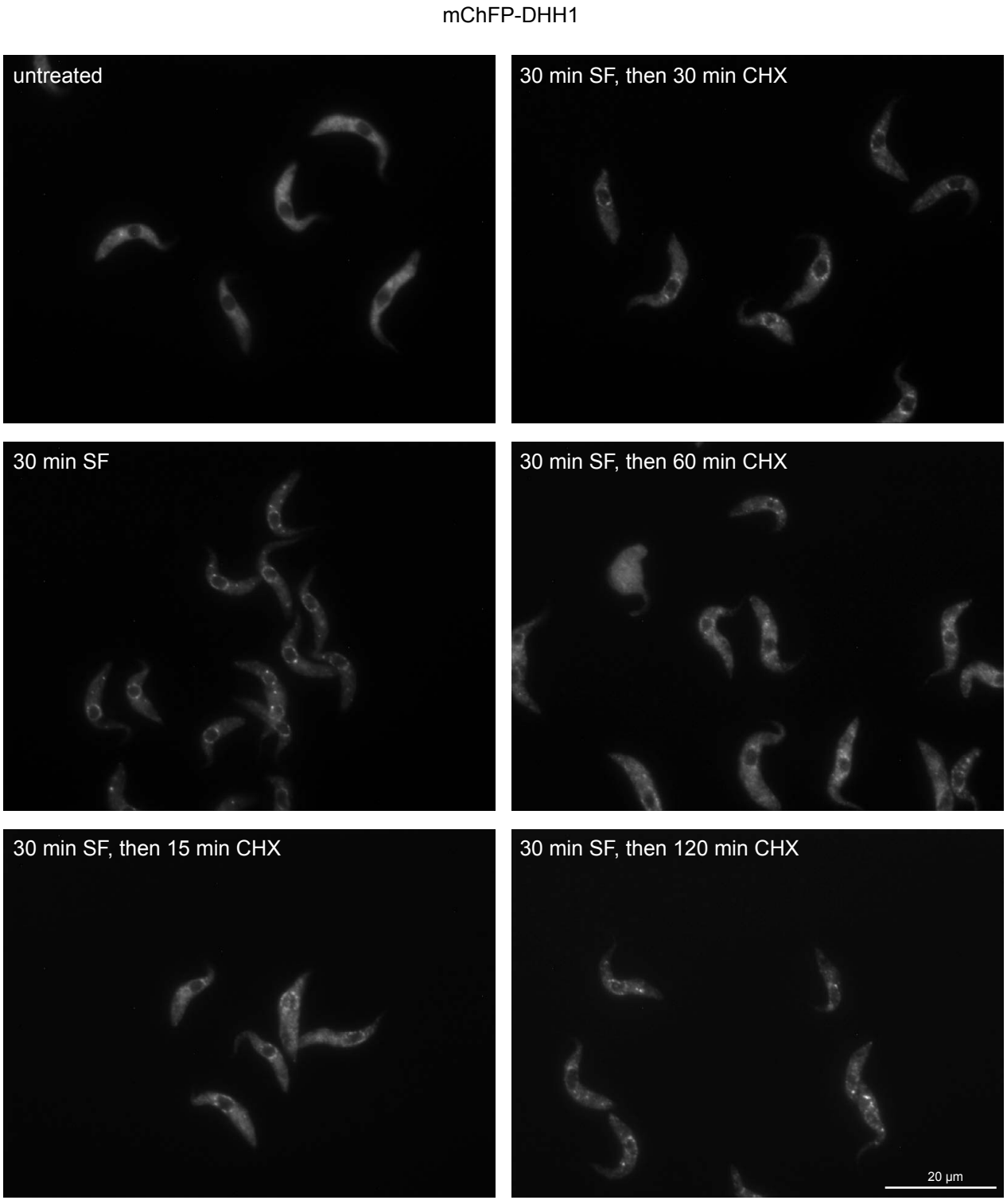
mChFP-DHH1
untreated
30 min SF, then 30 min CHX
30 min SF
30 min SF, then 60 min CHX
30 min SF, then 15 min CHX
30 min SF, then 120 min CHX
20 µm

B

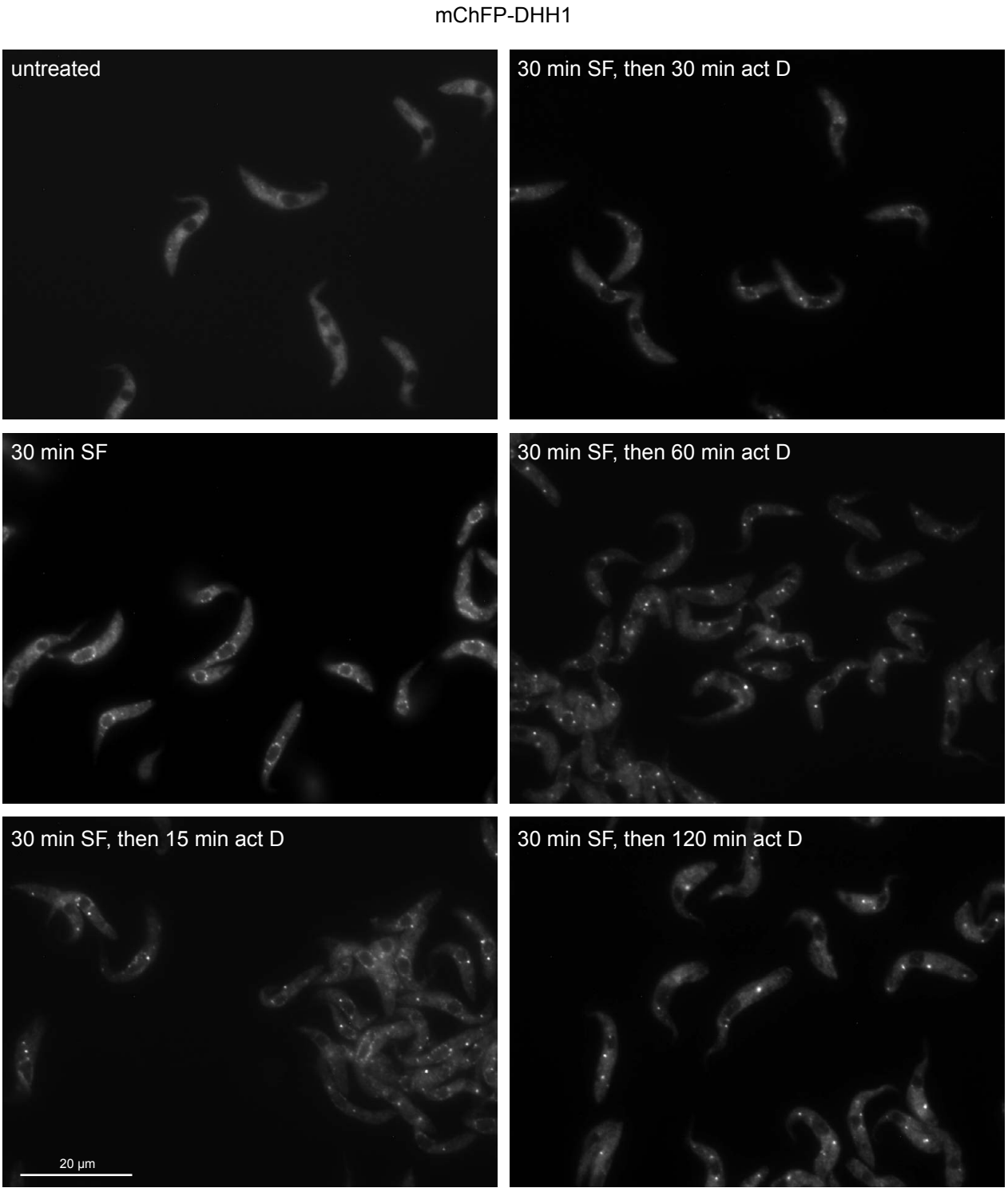

Figure S7
NPGs are stable in the presence of cycloheximide but not actinomycin D
Cells expressing mChFP-DHH1 were incubated with sinefungin (SF) for 30 minutes to induce the formation of NPGs. The effect of **(A)** cycloheximide and **(B)** actinomycin D (act D) on the NPGs was determined over a time-course.

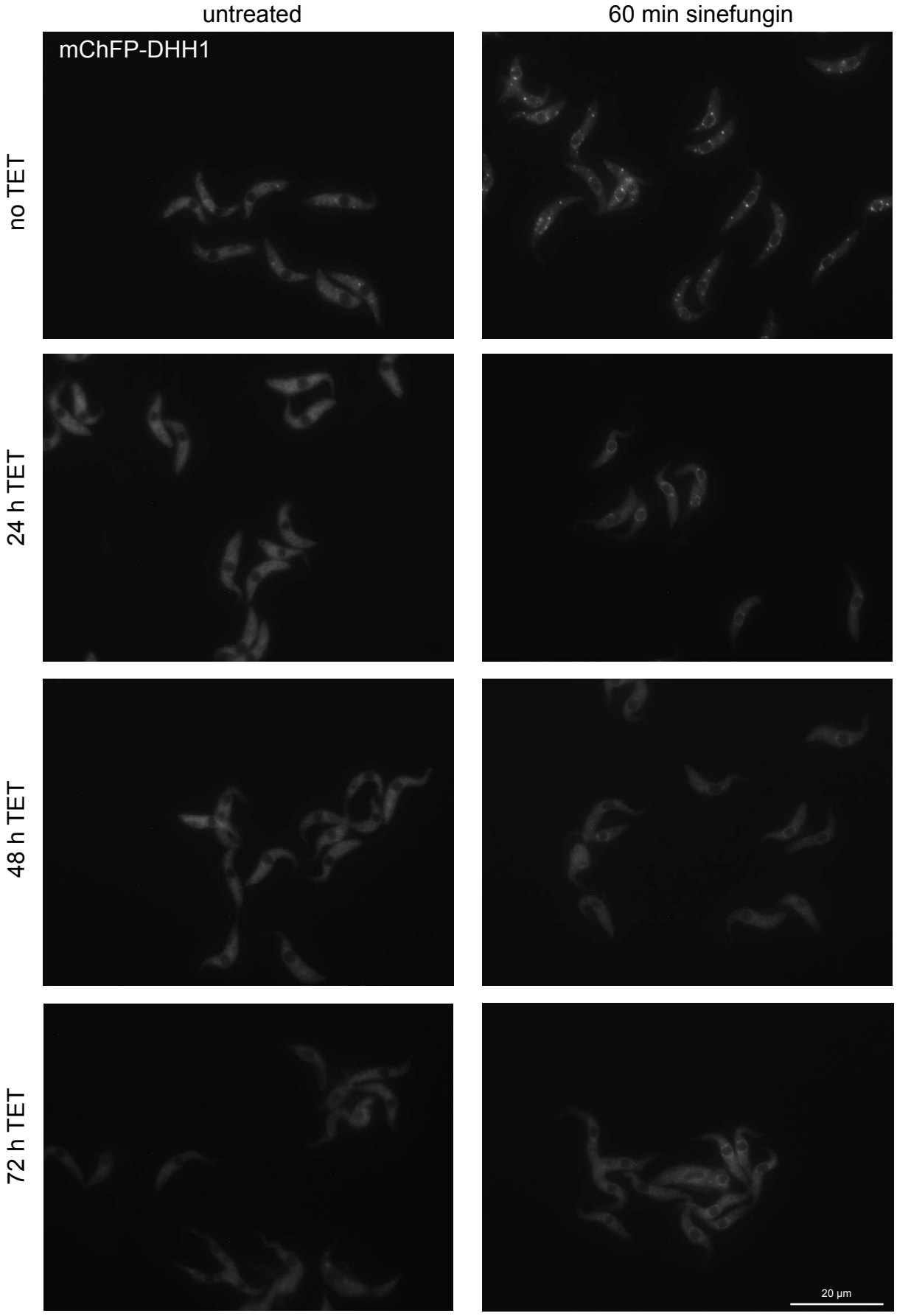

Figure S8
SCD6 RNAi depletion prevents P-body formation, but not the formation of NPGs
SCD6 was depleted in cells constitutively expressing mChFP-DHH1, a marker for both NPGs and P-bodies. The localization of mChFP-DHH1 protein to P-bodies and NPGs was monitored over a time-course of induction of SCD6 RNAi (compare with Figure 5).

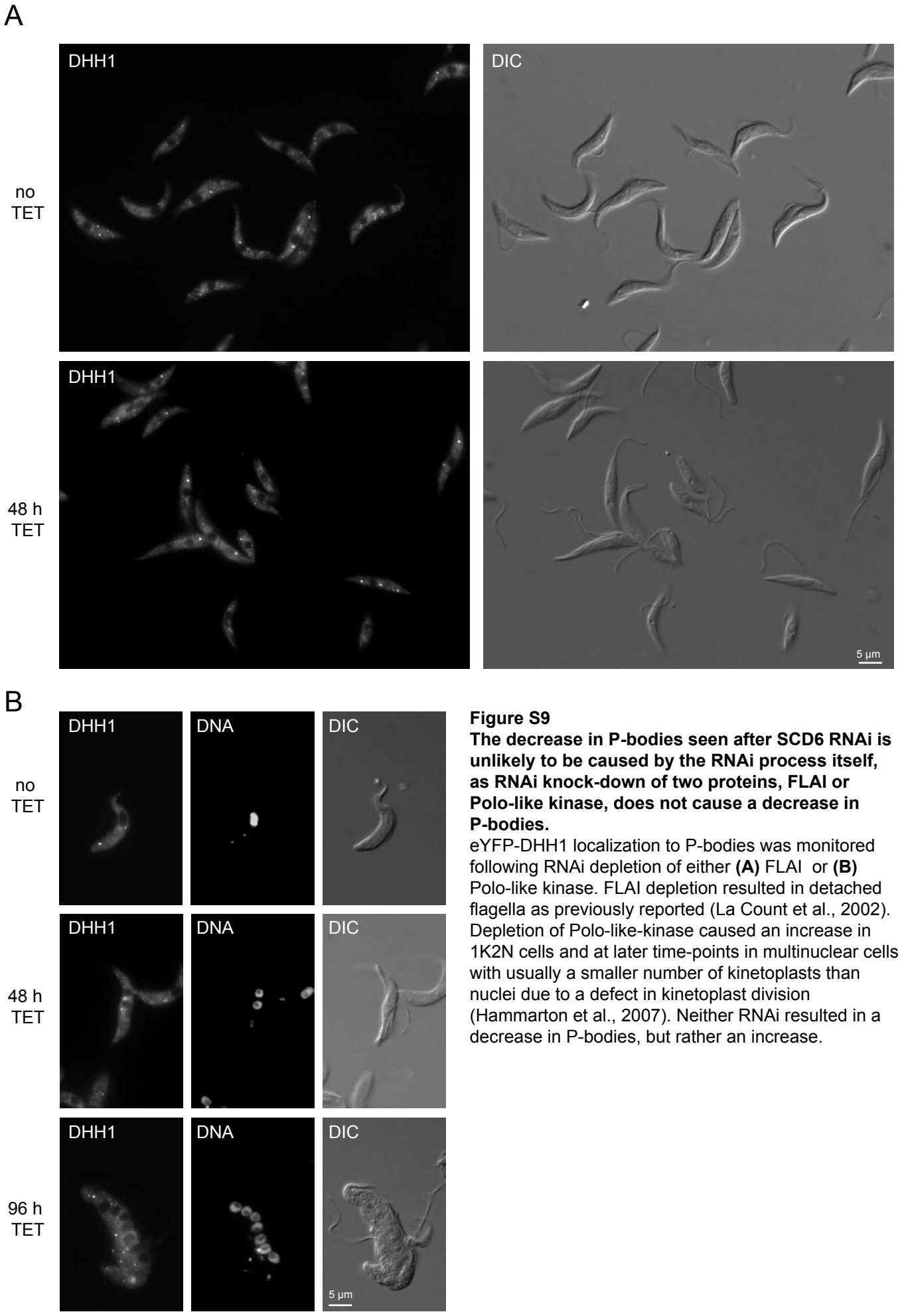

Figure S9
The decrease in P-bodies seen after SCD6 RNAi is unlikely to be caused by the RNAi process itself, as RNAi knock-down of two proteins, FLAI or Polo-like kinase, does not cause a decrease in P-bodies.
eYFP-DHH1 localization to P-bodies was monitored following RNAi depletion of either **(A)** FLAI or **(B)** Polo-like kinase. FLAI depletion resulted in detached flagella as previously reported (La Count et al., 2002). Depletion of Polo-like-kinase caused an increase in 1K2N cells and at later time-points in multinuclear cells with usually a smaller number of kinetoplasts than nuclei due to a defect in kinetoplast division (Hammarton et al., 2007). Neither RNAi resulted in a decrease in P-bodies, but rather an increase.

Table S1: Details of all plasmids used in this work. All backbone plasmids are described in Kelly et al., 2007 or Sunter et al., 2012, although in some cases a different selectable marker was used, as indicated.

	Gene ID	nucleotides of ORF used for targeting / RNAi / expression	restriction enzyme used for linearization	backbone plasmid	expression vector	selectable marker
SCD6-mChFP	Tb11.03.0530	219- end	SalI	p2705 with BSD	p3378	BSD
SCD6-mChFP	Tb11.03.0530	219- end	SalI	p2705	p2928	NEO
eYFP-DHH1	Tb927.10.3990	1-466	NheI	p2675 with BSD	p2829	BSD
mChFP-DHH1	Tb927.10.3990	1-466	NheI	p2679 with BSD	p2845	BSD
DRBD3-eYFP	Tb09.211.0560	132- end	Bst11071	p2710	p3216	NEO
DRBD4-eYFP	Tb11.01.5690	426- end	BamHI	p2710	p3217	NEO
CAF1-eYFP	Tb927.6.600	153- end	HpaI	p2710	p3218	NEO
PABP2-eYFP	Tb09.211.2150	539- end	XcmI	p2710	p3295	NEO
eIF4E1-eYFP	Tb11.18.0004	162- end	NruI	p2710	p3519	NEO
eIF4E2-eYFP	Tb927.10.16070	114- end	SexAI	p2710	p3520	NEO
eIF4E3-eYFP	Tb11.01.3630	249- end	BlpI	p2710	p3521	NEO
eIF4E4-eYFP	Tb927.6.1870	361- end	BspEI	p2710	p3522	NEO
CBP20-eYFP	Tb927.6.1970	112- end	Eco47III	p2710	p3523	NEO
eYFP-CGM1	Tb927.7.2080	1- 923	EcoRI	p2675	p3524	PURO
XPO1-eYFP	Tb11.01.5940	1841- end	AvaI	p2710	p3527	NEO
eIF4G3-eYFP	Tb927.8.4820	1319- end	BbsI	p2710	p3549	NEO
MEX67-eYFP	Tb11.22.0004	683- end	NheI	p2710	p3595	NEO
Nup62-eYFP	Tb927.4.5200	1659- end	EcoNI	p2710	p3596	NEO
Nup62-eYFP	Tb927.4.5200	1659- end	EcoNI	p2710 with HYG	p4063	HYG
Nup96-eYFP	Tb927.10.7060	1691- end	BsmI	p2710	p3597	NEO
Ran-binding protein 1-eYFP (putative)	Tb11.02.0870	232-end	AvaI	p2710	p4090	NEO
VASA-eYFP	Tb927.10.14550	1298- end	SfiI	p2710	p3675	NEO
XRNA-eYFP	Tb927.7.4900	3579- end	NheI	p2710	p3043	NEO
PABP1-eYFP	Tb09.211.0930	123- end	NsiI	p2710 with HYG	p2949	HYG
UPF1-eYFP	Tb927.5.2140	1704-end	BlpI	p2710 with HYG	P4181	HYG
Lsm5-eYFP	Tb927.6.4340	full length (inducible expression)	NotI	p2663	p2741	HYG
SmE-eYFP	Tb927.6.2700	full length	PshAI	p2710	p3871	NEO
SmE RNAi	Tb927.6.2700	full length	NotI	p3666	p3872	BSD
SCD6 RNAi	Tb11.03.0530	219-end	NotI	p3666	p3996	BSD
NUP158 RNAi	Tb11.03.0140	1659-2148	NotI	p3666	p4220	BSD
SCD6 inducible overexpression	Tb11.03.0530	full length	NotI	p3888	p3924	BSD
FlaI RNAi	as described in LaCount et al., 2002					